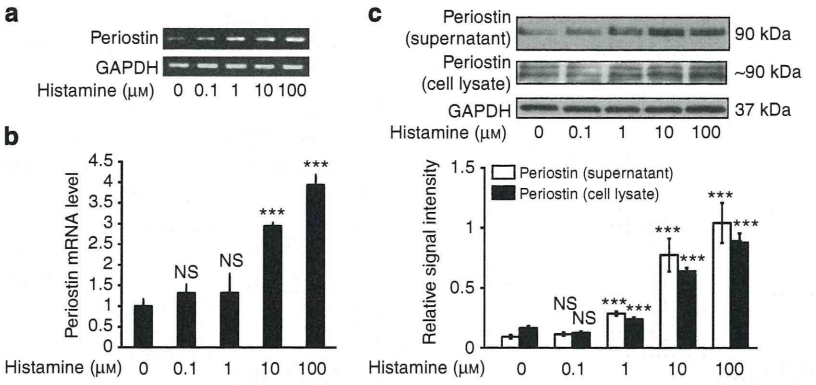

Figure 2. Periostin is upregulated upon histamine stimulation in cultured wild-type (WT) fibroblasts. WT fibroblasts were stimulated with histamine at the indicated concentrations for 2 hours (**a**, **b**) or 24 hours (**c**). Periostin mRNA expression was determined by reverse transcriptase–PCR (RT-PCR) analysis (**a**) and real-time PCR analysis (**b**). Periostin protein expression was evaluated by western blotting analysis (**c**). Three independent experiments were performed, and representative blots and quantitative analysis of signal density on blots from three independent experiments are shown (using glyceraldehyde 3-phosphate dehydrogenase (GAPDH) as an internal control). Values in **b** and **c** are shown as mean ± SD for three independent experiments. ***$P<0.001$; NS, no significance, compared with control (0 μM histamine) by one-way analysis of variance (ANOVA) followed by Dunnett's test.

but not by either H2R or H4R antagonists (Figure 3a and b), suggesting that histamine upregulates periostin expression through H1R activation *in vitro*.

Next, we determined whether periostin was induced by histamine via H1R *in vivo*. Histamine release was triggered through mast cell degranulation using the compound 48/80 in WT and H1R-deficienct ($H1R^{-/-}$) mice. After treatment with compound 48/80 for three consecutive days, skin at the injected site was sampled. Periostin expression in WT and $H1R^{-/-}$ mouse skin was compared by western blotting analyses (Figure 3c). In WT mice, periostin expression markedly increased after compound 48/80 treatment, although no such increase was observed in $H1R^{-/-}$ mice (Figure 3c). These results suggest that H1R mediates histamine-induced periostin upregulation.

H1R activation upregulates periostin expression via the ERK1/2 pathway

Next, to investigate the signal transduction pathway involved after H1R activation by histamine in dermal fibroblasts, we used a commercial human phosphorylated kinase array kit to profile the phosphorylated kinases in normal human dermal fibroblasts (Figure 4a). Subsequently, phosphorylation of analogous kinases was confirmed in murine dermal fibroblasts by western blot analysis (Figure 4b). Compared with nontreated dermal fibroblasts, enhanced phosphorylation of extracellular signal-regulated kinase 1/2 (ERK1/2) and the downstream factor cAMP response element-binding protein (CREB) was observed after 10 minutes and 30 minutes of histamine stimulation (Figure 4a and b).

Furthermore, we found that histamine-induced phosphorylation of ERK1/2 and CREB was blocked not only with U0126 (a selective ERK1/2 kinase inhibitor) but also with an H1R antagonist (Figure 4c and d).

These observations demonstrated that histamine activates the ERK1/2 signal transduction pathway via H1R in dermal fibroblasts.

In addition, to verify the involvement of ERK1/2 activation in histamine-induced upregulation of periostin, western blotting analysis was performed (Figure 4c and d). Both U0126 and H1R antagonists decreased the expression of periostin, as well as suppressed the phosphorylation of CREB (Figure 4c and d). These results indicated that H1R-mediated signaling upregulated periostin expression via the ERK1/2 pathway.

H1R-mediated upregulation of periostin is essential for histamine-induced collagen production

To investigate the involvement of periostin in histamine-induced collagen production, primary dermal fibroblasts from WT and periostin-deficient ($PN^{-/-}$) mice were stimulated with histamine (100 μM) for 48 hours. The induction of collagen was abolished in $PN^{-/-}$ fibroblasts at both the mRNA (Figure 5a) and protein (Figure 5b and c) levels. Histamine-treated $PN^{-/-}$ fibroblasts did not exhibit increases in mRNA or protein expression of type I collagen (Col1; Figure 5a–c).

As described above, periostin was induced by histamine via the H1R pathway. To further clarify whether H1R was associated with histamine-induced collagen production, H1R antagonist was added to WT fibroblasts before histamine stimulation. After 48 hours of histamine stimulation, collagen production was evaluated as determined by quantitative real-time reverse transcriptase–PCR, Sircol Collagen Assay, and western blotting analyses (Figure 6). As expected, histamine-induced collagen synthesis was blocked by an H1R antagonist (Figure 6a–c). Furthermore, this inhibitory effect was rescued by the addition of recombinant mouse periostin (rmPeriostin; Figure 6a–c).

In addition, this mechanism was confirmed in cultured primary human dermal fibroblasts derived from healthy donor skin biopsies (Supplementary Figure S1 online).

Finally, we addressed the question of how strong the effect of histamine on tissue remodeling was in AD. Compared with normal skin and AD nonlesioned skin, increased expression of

periostin was observed in both acute AD lesioned skin and skin tissues with positive *Dermatophagoides farinae* (Derf1) scratch tests (Supplementary Figure S2 online). Our results suggest that histamine may contribute to the initiation of tissue remodeling during the acute phase of AD.

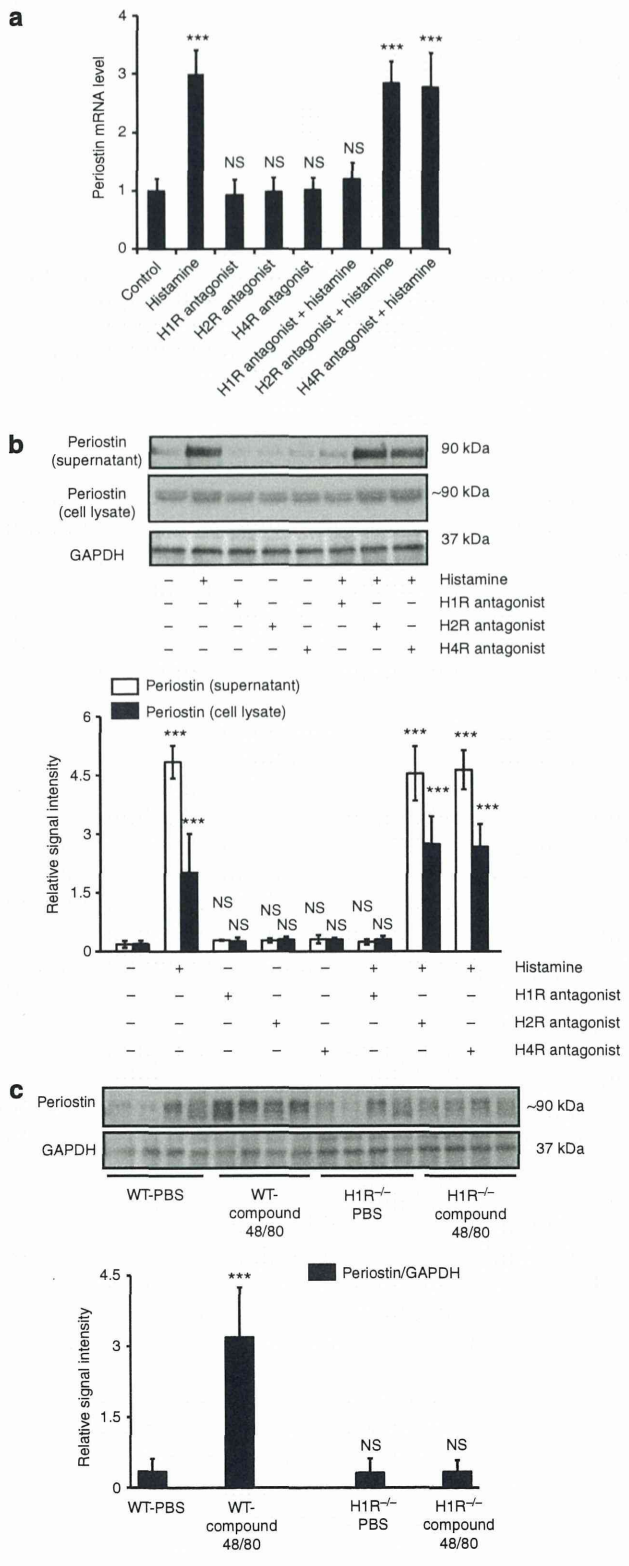

DISCUSSION

Here, we report that histamine increases the expression of periostin in dermal fibroblasts. Moreover, periostin increases *de novo* synthesis of Col1 via an ERK1/2-mediated pathway.

It is widely recognized that mast cells contribute to the healing of skin wounds (Hebda *et al.*, 1993; Artuc *et al.*, 1999; Trautmann *et al.*, 2000; Gailit *et al.*, 2001; Noli and Miolo, 2001). Impaired wound closure in mast cell–deficient mice indicates that mast cells have a crucial role in the wound repair process (Weller *et al.*, 2006). An increased number of mast cells in fibrotic tissues such as scleroderma, keloid, or healing wounds has been identified (Hawkins *et al.*, 1985; Atkins and Clark, 1987), although it is still unclear whether mast cells are fibrogenic. In many instances, chemical mediators, such as histamine, which is derived from degranulated mast cells or basophils, have been implicated as a cause of inflammation and tissue remodeling in AD (Davies and Greaves, 1980; Nishioka *et al.*, 1987; Wahlgren, 1999; Murota and Katayama, 2009). In support of these findings, H1R antagonist has been shown to inhibit the synthesis of Col1 by dermal fibroblasts (Murota *et al.*, 2008). Interestingly, histamine H1R antagonists but not H2R antagonists reduced wound closure in experimentally induced skin wounds in mice (Weller *et al.*, 2006). Therefore, histamine is believed to have an important role in the wound-healing process. Indeed, disruption of histamine in histidine decarboxylase knockout mice resulted in delayed cutaneous would healing, and this phenotype was rescued by exogenous histamine administration (Numata *et al.*, 2006). It remains unclear how histamine promotes wound healing. Some reports indicated that histamine induces fibroblast proliferation after a long period of coculturing (Russel *et al.*, 1977; Topol *et al.*, 1981). In our study, increased expression of Col1 mRNA was observed after 48 hours of co-incubation with histamine. Thus, histamine-mediated tissue remodeling may require the expression of periostin as a second messenger in order to elicit tissue remodeling.

Figure 3. Histamine upregulates periostin expression via histamine receptor 1 (H1R) *in vitro* and *in vivo*. *In vitro*, wild-type (WT) fibroblasts were either treated with histamine antagonists (H1R, H2R, or H4R; 100 mM) or left untreated for 2 hours, and then cells were stimulated with histamine (100 μM) for an additional 2 hours (**a**) or 24 hours (**b**). Periostin expression was examined by quantitative real-time reverse transcriptase–PCR (qRT-PCR) (**a**) and western blotting analysis (**b**). *In vivo*, WT and *H1*$^{-/-}$ mice were treated with mast cell stimulator compound 48/80 for 3 days by subcutaneous injection, and periostin protein expression in the injected site skin was evaluated by western blotting analysis ($n=4$ mice per group); representative blots and quantitative analysis of signal density on blots from four mice of each group are shown (using glyceraldehyde 3-phosphate dehydrogenase (GAPDH) as an internal control). (**c**) Values in **a** and **b** are shown as mean ± SD for three independent experiments. Values in **c** are shown as mean ± SD for blot signals from four mice. ***$P<0.001$; NS, no significance, compared with control (0 μM histamine in **a** and **b**; WT-phosphate-buffered saline in **c** by one-way analysis of variance (ANOVA) followed by Dunnett's test.

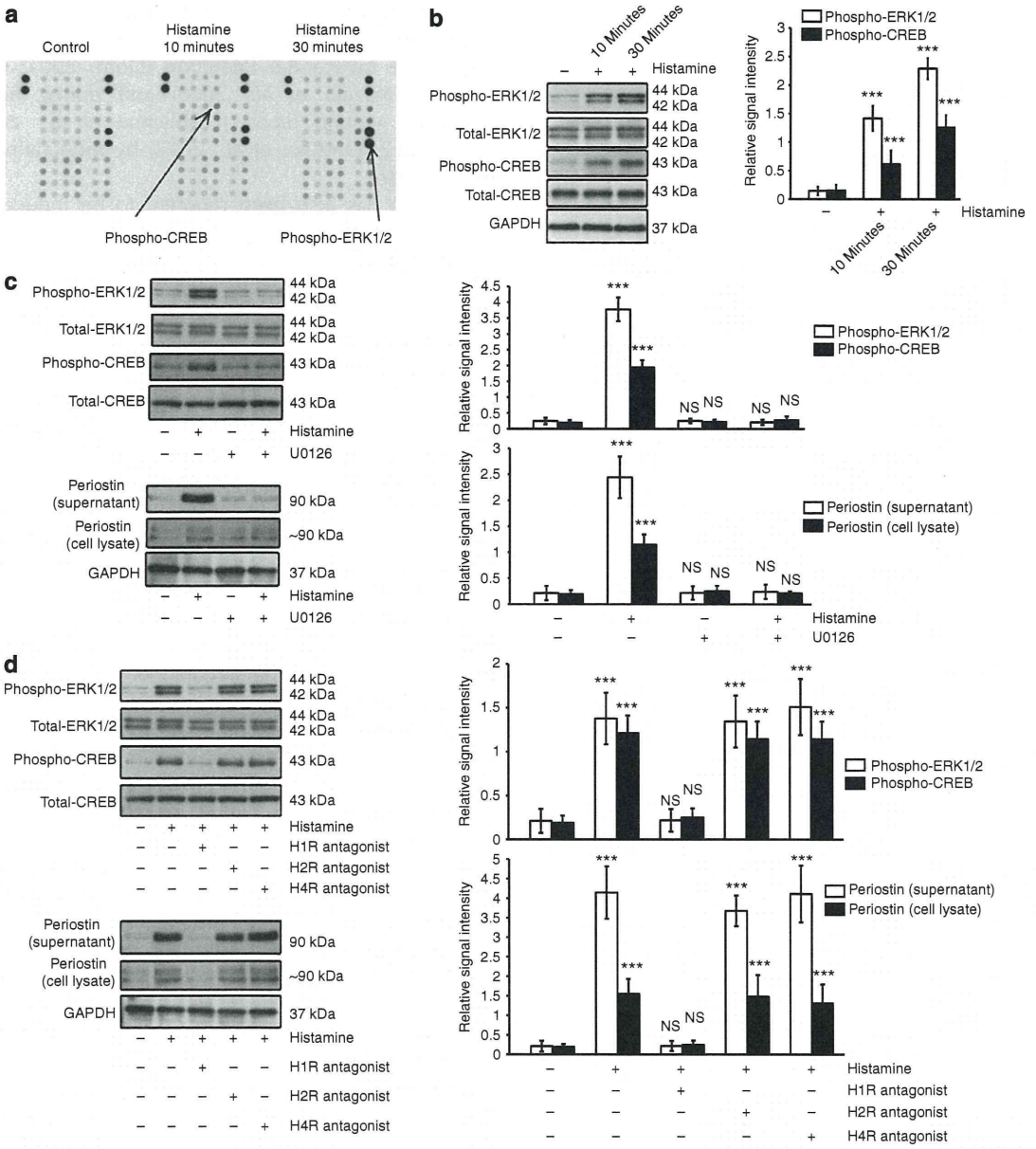

Figure 4. Histamine receptor 1 (H1R) activation upregulates periostin expression via the extracellular signal-regulated kinase 1/2 (ERK1/2) pathway. (**a**) The phosphorylation state was detected by R&D Systems Proteome Profiler Phospho-Kinase Array in normal human dermal fibroblasts, which were either untreated or treated with histamine for 10 minutes or 30 minutes. The activated kinases are indicated by arrows. (**b**) Phosphorylated ERK1/2 and phosphorylated cAMP response element-binding protein (CREB) were evaluated by western blotting analyses in murine wild-type (WT) fibroblasts following histamine stimulation for 10 minutes and 30 minutes. (**c**) WT fibroblasts with or without ERK1/2 inhibitor (U0126, 20 μM) preincubation were stimulated with histamine (30 minutes, upper panel; 24 hours, lower panel). Phosphorylated ERK1/2, phosphorylated CREB, and periostin protein expression was examined by western blotting analyses. (**d**) WT fibroblasts cultured in the presence or absence of preincubation with histamine receptor antagonists (H1R, H2R, or H4R; 100 mM) were stimulated with histamine (30 minutes, upper panel; 24 hours, lower panel). Phosphorylated ERK1/2, phosphorylated CREB, and periostin protein expression was examined by western blotting analyses. Three independent experiments were performed, and representative blots and quantitative analysis of signal density on blots from three independent experiments are shown (using glyceraldehyde 3-phosphate dehydrogenase (GAPDH) as an internal control). ***$P<0.001$; NS, no significance, compared with control (0 μM histamine) by one-way analysis of variance (ANOVA) followed by Dunnett's test.

Periostin, a recently characterized matricellular protein, has been reported to have crucial roles in tooth and periodontium development (Horiuchi *et al.*, 1999), cancer proliferation and invasion (Siriwardena *et al.*, 2006; Baril *et al.*, 2007; Kudo *et al.*, 2012), cardiac healing after acute myocardial infarction (Shimazaki *et al.*, 2008), idiopathic interstitial pneumonia (Okamoto *et al.*, 2011), and bone marrow fibrosis (Oku *et al.*, 2008). Furthermore, periostin is highly expressed in connective tissue and at the remodeling tissue site after injury or inflammation. This protein is secreted from fibroblasts via

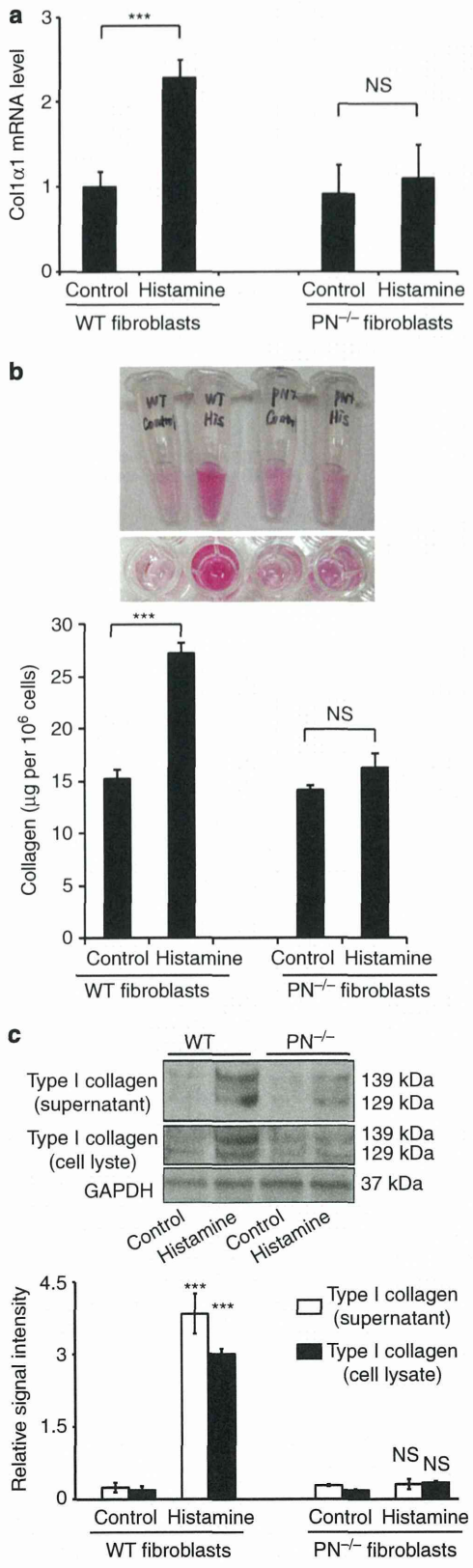

transforming growth factor beta stimulation (Horiuchi *et al.*, 1999). Periostin was shown to accelerate cardiac healing after acute myocardial infarction (Dorn, 2007; Oka *et al.*, 2007; Shimazaki *et al.*, 2008) and during full-thickness cutaneous wound repair (Nishiyama *et al.*, 2011; Elliott *et al.*, 2012; Ontsuka *et al.*, 2012) by modulating fibroblast differentiation.

Periostin has also been reported to be induced by other factors, including bone morphogenetic proteins, vascular endothelial growth factor, connective tissue growth factor, vitamin K, IL-3, IL-4, IL-6, and IL-13 (Asano *et al.*, 2005; Takayama *et al.*, 2006; Iekushi *et al.*, 2007; Blanchard *et al.*, 2008; Coutu *et al.*, 2008; Banerjee *et al.*, 2009; Norris *et al.*, 2009). Recently, the increased expression of periostin was confirmed in various allergic diseases such as bronchial asthma (Takayama *et al.*, 2006), AD (Masuoka *et al.*, 2012), and eosinophilic chronic rhinosinusitis (Hur *et al.*, 2012). As an IL-4- and IL-13-inducible protein, periostin is associated with tissue remodeling in bronchial asthma (Takayama *et al.*, 2006), allergic eosinophilic esophagitis (Blanchard *et al.*, 2008), AD (Masuoka *et al.*, 2012), and allergic rhinitis (Hur *et al.*, 2012). In the present study, histamine was found to directly induce periostin expression, whereas the expression levels of transforming growth factor beta, IL-4, and IL-13 were not altered by histamine stimulation (data not shown). Thus, we postulate that periostin is involved in the initiation of tissue remodeling in chronic allergic diseases.

AD is known to develop tissue remodeling, which is characterized by epidermal thickening, hyperkeratosis and fibrosis of the papillary dermis, increased fibroblast proliferation, and collagen accumulation, and these features are caused by nonspecific stimuli, constant scratching, and rubbing (Lee *et al.*, 2009). Tissue remodeling and repair are thought to be the underlying causes of chronic allergic inflammation, such as in asthmatic diseases and AD (Leung, 1995). Recently, increased expressions of periostin and the inducers of periostin (IL-4, IL-13, and transforming growth factor beta) were identified in a screening of AD-associated genes in genome-wide association studies and quantitative mRNA expression analysis in lesion tissues (Hoffjan and Epplen, 2005; Wood *et al.*, 2009a, 2009b). Furthermore, in the present study, elevated expression of periostin was found in lesional skin of patients with AD. These results suggest that periostin may be involved in AD and in asthma.

Figure 5. Periostin is essential in histamine-induced collagen production *in vitro*. Primary dermal fibroblasts from wild type (WT) and periostin-deficienct ($PN^{-/-}$) mice were stimulated with histamine (100 μM) or phosphate-buffered saline (PBS) (control) for 48 hours. The collagen type-I alpha 1 (Col1α1) mRNA level was examined by quantitative real-time reverse transcriptase–PCR (qRT-PCR) (**a**), and collagen protein expression was evaluated by Sircol assay (**b**) and western blotting analysis; representative blots and quantitative analysis of signal density on blots from three independent experiments are shown (using glyceraldehyde 3-phosphate dehydrogenase (GAPDH) as an internal control) (**c**). Values are shown as mean ± SD for three independent experiments. ***$P<0.001$; NS, no significance, compared with paired control (WT fibroblasts control or $PN^{-/-}$-fibroblasts control) by Student's *t*-test.

In WT and $PN^{-/-}$ mice, a mite extract–induced AD model was established and analyzed. In contrast to WT mice, $PN^{-/-}$ mice showed amelioration of epidermal hyperplasia and inflammatory cell infiltration (Masuoka *et al.*, 2012). Moreover, periostin directly induces production of thymic stromal lymphoprotein in keratinocytes (Masuoka *et al.*, 2012). Thus, periostin was suggested to have a critical role in the amplification and chronicity of allergic skin inflammation.

The results of the present study demonstrate the role of periostin in histamine-mediated collagen production. We found that H1R-mediated phosphorylation of ERK1/2 had a crucial role in histamine-induced collagen production. These observations may open a new window of therapeutic opportunity against airway remodeling in asthma or dermal remodeling in AD, as histamine H1R anatagonists are expected to ameliorate tissue remodeling.

As refractory chronic allergic symptoms are known to impair the quality of life, work productivity, and overall activity (Meltzer *et al.*, 1999; Thompson *et al.*, 2000; Kawashima *et al.*, 2002; Baiardini *et al.*, 2003; Spector *et al.*, 2007), we believe that these studies will provide a basis for exploring the fibrotic components of allergic diseases in skin and other tissues.

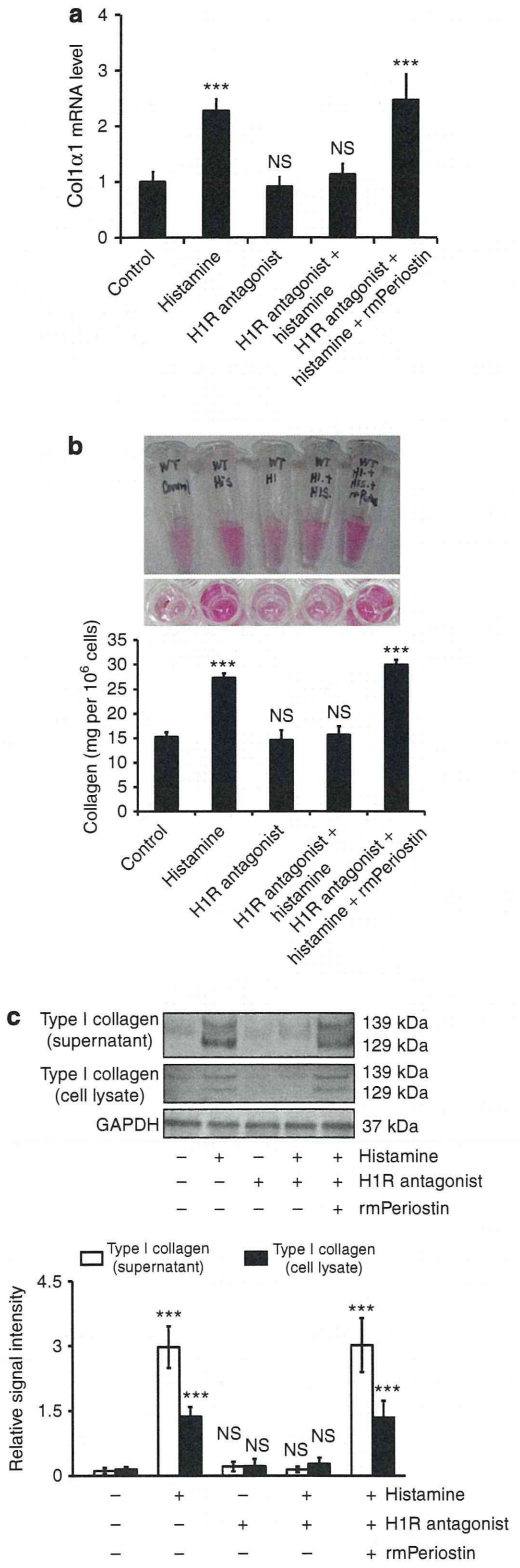

MATERIALS AND METHODS

Mice

WT mice (C57BL/6 strain) were purchased from CLEA Japan (Osaka, Japan). Periostin gene knockout ($PN^{-/-}$) mice (C57BL/6 strain) were generated as previously described.(Shimazaki and Kudo, 2008) Histamine receptor 1 gene knockout ($H1R^{-/-}$) mice (C57BL/6 strain) were purchased from Oriental Bio Service (Kyoto, Japan). Mice were maintained in our pathogen-free animal facility. Animal care and experimentation were performed in accordance with the institutional guidelines of the National Institute of Biomedical Innovation, Osaka, Japan and Osaka University, Osaka, Japan. Six-week-old male mice were used in all experiments. All experiments used four mice per group.

Compound 48/80 treatment

Compound 48/80 (Sigma, St Louis, MO) was dissolved in phosphate-buffered saline at a concentration of 1 mg ml^{-1} and sterilized by filtration. With the use of a 27-gauge needle, 100 µl of compound 48/80 or phosphate-buffered saline was subcutaneously injected into the back side of mice each day for 3 days. One day after the final injection, the skin at the injected site was removed and solubilized at 4 °C in lysis buffer (0.5% sodium deoxycholate, 1% Nonidet P40,

Figure 6. Histamine receptor 1 (H1R)-mediated upregulation of periostin is essential in histamine-induced collagen production. Wild-type (WT) fibroblasts cultured with or without H1R antagonist preincubations were stimulated with histamine (100 µM) alone or in the presence of recombinant mouse periostin (rmPeriostin, 100 ng/ml^{-1}). The collagen type-I alpha 1 (Col1α1) mRNA level was examined by quantitative real-time reverse transcriptase–PCR (qRT-PCR) (**a**), and collagen protein expression was evaluated by Sircol assay (**b**) and western blotting analysis; representative blots and quantitative analysis of signal density on blots from three independent experiments are shown (using glyceraldehyde 3-phosphate dehydrogenase (GAPDH) as an internal control) (**c**). Values are shown as mean ± SD for three independent experiments. ***$P<0.001$; NS, no significance compared with control (0 µM histamine) according to one-way analysis of variance (ANOVA) followed by Dunnett's test.

0.1% sodium dodecyl sulfate, 100 μg ml^{-1} phenylmethylsulfonyl fluoride, 1 mM sodium orthovanadate, and protease inhibitor cocktail) for western blotting analysis.

Cell culture

Murine primary dermal fibroblasts from the skin of four newborn WT and four newborn *PN*$^{-/-}$ mice were isolated and cultured as previously described (Terao *et al.*, 2010). Human primary dermal fibroblasts were purchased from DS Pharma Biomedical (Osaka, Japan). After 24 hours of serum starvation, dermal fibroblasts at confluence were treated with 0.1 to 100 μM histamine (Sigma–Aldrich, Tokyo, Japan) or 100 ng ml^{-1} recombinant mouse periostin (rmPeriostin, R&D Systems, Minneapolis, MN) for the indicated periods of time before extraction of RNA and protein. Cells were used at passage three. In each experiment, the obtained fibroblasts were examined at the same time point and under the same culture conditions (e.g., cell density, passage, and days after plating). For inhibition experiments, fibroblasts were preincubated for 2 hours with specific histamine receptor antagonists (Pyrilamine maleate, Cimetidine, JNJ7777120, 100 mM, Sigma–Aldrich) or ERK1/2 inhibitor (U0126, 20 μM, Cell Signaling Technology, Beverly, MA) before the addition of histamine. We performed serial dilutions of each agent to identify the most effective concentrations to be used in the experiments, as determined by MTT assays and western blotting analyses.

Quantitative real-time and direct reverse transcriptase–PCR analysis of mRNA

Total RNA was isolated from fibroblasts using the RNeasy Mini Kit (QIAGEN, Tokyo, Japan) according to the manufacturer's protocol. First, 100 ng of RNA was reverse-transcribed using the QuantiTect Reverse Transcription Kit (QIAGEN). For quantitative real-time reverse transcriptase–PCR analysis, standard curves for periostin, collagen, and glyceraldehyde 3-phosphate dehydrogenase (GAPDH) were generated from serial dilutions of positively expressing cDNA. Relative quantification of the PCR products was carried out using the ABI prism 7000 (Applied Biosystems, Darmstadt, Germany) and the comparative threshold cycle (C_T) method. The "fold-induction" was calculated as the ratio to values of cells that were not incubated with histamine or periostin. The primers used for real-time PCR were as follows: periostin, sense 5′-GAACGAATCATTACAGGTCC-3′, antisense 5′-GGAGACCTCTTTTTGCAAGA-3′; collagen type-I alpha 1 (Col1-α1), sense 5′-GAGCCCTCGCTTCCGTACTC-3′, antisense 5′-TGTTCCCTACTCAGCCGTCTGT-3′; and GAPDH, sense 5′-TGTC ATCATACTTGGCAGGTTTCT-3′, antisense 5′-CATGGCCTTCCGTG TTCCTA-3′. Each reaction was performed in triplicate. Variation within samples was less than 10%. Statistical analysis was performed with the Student's paired *t*-test.

Western blotting analyses

For preparation of protein samples, cell pellets and skin samples were extracted as described above, and 5 μg of extracted protein was used for western blotting analysis, as described previously (Terao *et al.*, 2010). The primary antibodies were used at the following dilutions: anti-type I collagen (Calbiochem, San Diego, CA) at 1:500, anti-periostin (R&D Systems, Minneapolis, MN) at 1:500, anti-phospho-ERK1/2 (Cell Signaling Technology) at 1:1,000, anti-total ERK1/2 (Cell Signaling Technology) at 1:1,000, anti-phospho-CREB (Cell Signaling Technology) at 1:1,000, anti-total CREB (Cell Signaling Technology) at 1:1,000, and anti-GAPDH (Santa Cruz Biotechnology, Santa Cruz, CA) at 1:500. Staining with the anti-GAPDH antibody was used as a loading control. Signal intensity of bands was quantified using the ImageJ densitometry software (http://rsb.info.nih.gov/ij/index.html) and normalized to GAPDH signal intensity.

Sircol collagen assay

The soluble collagen levels in culture supernatants were measured using a Sircol Collagen Assay (Biocolor, Belfast, UK). This assay measured total secreted collagen from cultured cells. Briefly, cells were cultured for 48 hours with or without treatment, and then supernatants were collected. One milliliter of Sirius red, an anionic dye that specifically reacts with the basic side chain groups of collagens, was added to 200 μl of the supernatant and incubated with gentle rotation for 30 minutes at room temperature. After centrifugation, the collagen-bound dye was resolubilized in 1 ml of 0.5 M NaOH, and the absorbance at 540 nm was measured.

Phosphorylated kinase array

Phosphorylated kinase was profiled with the Proteome Profiler Human Phospho-Kinase Array Kit (R&D Systems). The procedures were performed according to the manufacturer's protocol using 300 μg of protein lysate per array.

Statistical analysis

All experiments reported in this paper were repeated at least three times, yielding similar results, and data are presented as mean ± SD. The Student's two-tailed *t*-test (Microsoft Excel software, Redmond, WA) was used for comparison between two groups. When analysis included more than two groups, one-way analysis of variance (ANOVA) followed by Dunnett's test was used. *P*-values less than 0.05 were considered statistically significant.

CONFLICT OF INTEREST

The authors state no conflict of interest.

ACKNOWLEDGMENTS

We thank Kenju Nishida for excellent technical support. This study was partly supported by a research grant from the Ministry of Health, Labour and Welfare, Japan.

SUPPLEMENTARY MATERIAL

Supplementary material is linked to the online version of the paper at http://www.nature.com/jid

REFERENCES

Artuc M, Hermes B, Steckelings UM *et al.* (1999) Mast cells and their mediators in cutaneous wound healing–active participants or innocent bystanders? *Exp Dermatol* 8:1–16

Asano M, Kubota S, Nakanishi T *et al.* (2005) Effect of connective tissue growth factor (CCN2/CTGF) on proliferation and differentiation of mouse periodontal ligament-derived cells. *Cell Commun Signal* 3:11

Atkins FM, Clark RA (1987) Mast cells and fibrosis. *Arch Dermatol* 123:191–3

Baiardini I, Giardini A, Pasquali M *et al.* (2003) Quality of life and patients' satisfaction in chronic urticaria and respiratory allergy. *Allergy* 58:621–3

Banerjee I, Fuseler JW, Intwala AR *et al.* (2009) IL-6 loss causes ventricular dysfunction, fibrosis, reduced capillary density, and dramatically alters the cell populations of the developing and adult heart. *Am J Physiol Heart Circ Physiol* 296:H1694–704

Baril P, Gangeswaran R, Mahon PC *et al.* (2007) Periostin promotes invasiveness and resistance of pancreatic cancer cells to hypoxia-induced cell death: role of the beta4 integrin and the PI3k pathway. *Oncogene* 26:2082–94

Blanchard C, Mingler MK, McBride M *et al.* (2008) Periostin facilitates eosinophil tissue infiltration in allergic lung and esophageal responses. *Mucosal Immunol* 1:289–96

Cohen IK, Beaven MA, Horáková Z *et al.* (1972) Histamine and collagen synthesis in keloid and hypertrophic scar. *Surg Forum* 23:509–10

Coutu DL, Wu JH, Monette A *et al.* (2008) Periostin, a member of a novel family of vitamin K-dependent proteins, is expressed by mesenchymal stromal cells. *J Biol Chem* 283:17991–8001

Davies MG, Greaves MW (1980) Sensory responses of human skin to synthetic histamine analogues and histamine. *Br J Clin Pharmacol* 9:461–5

Dorn GW (2007) Periostin and myocardial repair, regeneration, and recovery. *N Engl J Med* 357:1552–4

Elliott CG, Wang J, Guo X *et al.* (2012) Periostin modulates myofibroblast differentiation during full-thickness cutaneous wound repair. *J Cell Sci* 125:121–32

Gailit J, Marchese MJ, Kew RR *et al.* (2001) The differentiation and function of myofibroblasts is regulated by mast cell mediators. *J Invest Dermatol* 117:1113–9

Hawkins RA, Claman HN, Clark RA *et al.* (1985) Increased dermal mast cell populations in progressive systemic sclerosis: a link in chronic fibrosis? *Ann Intern Med* 102:182–6

Hebda PA, Collins MA, Tharp MD (1993) Mast cell and myofibroblast in wound healing. *Dermatol Clin* 11:685–96

Hoffjan S, Epplen JT (2005) The genetics of atopic dermatitis: recent findings and future options. *J Mol Med (Berl)* 83:682–92

Horiuchi K, Amizuka N, Takeshita S *et al.* (1999) Identification and characterization of a novel protein, periostin, with restricted expression to periosteum and periodontal ligament and increased expression by transforming growth factor beta. *J Bone Miner Res* 14:1239–49

Hur DG, Khalmuratova R, Ahn SK *et al.* (2012) Roles of periostin in symptom manifestation and airway remodeling in a murine model of allergic rhinitis. *Allergy Asthma Immunol Res* 4:222–30

Iekushi K, Taniyama Y, Azuma J *et al.* (2007) Novel mechanisms of valsartan on the treatment of acute myocardial infarction through inhibition of the antiadhesion molecule periostin. *Hypertension* 49:1409–14

Kawashima M, Harada S, Tango T (2002) Review of fexofenadine in the treatment of chronic idiopathic urticaria. *Int J Dermatol* 41:701–6

Kudo Y, Iizuka S, Yoshida M *et al.* (2012) Periostin directly and indirectly promotes tumor lymphangiogenesis of head and neck cancer. *PLoS One* 7:e44488

Lee JH, Chen SY, Yu CH *et al.* (2009) Noninvasive *in vitro* and *in vivo* assessment of epidermal hyperkeratosis and dermal fibrosis in atopic dermatitis. *J Biomed Opt* 14:014008

Leung DY (1995) Atopic dermatitis: the skin as a window into the pathogenesis of chronic allergic diseases. *J Allergy Clin Immunol* 96:302–18

Masuoka M, Shiraishi H, Ohta S *et al.* (2012) Periostin promotes chronic allergic inflammation in response to Th2 cytokines. *J Clin Invest* 122:2590–600

Meltzer EO, Casale TB, Nathan RA *et al.* (1999) Once-daily fexofenadine HCl improves quality of life and reduces work and activity impairment in patients with seasonal allergic rhinitis. *Ann Allergy Asthma Immunol* 83:311–7

Murakami T, Yoshioka M, Yumoto R *et al.* (1998) Topical delivery of keloid therapeutic drug, tranilast, by combined use of oleic acid and propylene glycol as a penetration enhancer: evaluation by skin microdialysis in rats. *J Pharm Pharmacol* 50:49–54

Murota H, Bae S, Hamasaki Y *et al.* (2008) Emedastine difumarate inhibits histamine-induced collagen synthesis in dermal fibroblasts. *J Invest Allergol Clin Immunol* 18:245–52

Murota H, Katayama I (2009) Emedastine difumarate: a review of its potential ameliorating effect for tissue remodeling in allergic diseases. *Expert Opin Pharmacother* 10:1859–67

Nishioka K, Katayama I, Doi T (1987) Histamine release by scratching inflamed skin. *J Dermatol* 14:284–5

Nishiyama T, Kii I, Kashima TG *et al.* (2011) Delayed re-epithelialization in periostin-deficient mice during cutaneous wound healing. *PLoS One* 6:e18410

Noli C, Miolo A (2001) The mast cell in wound healing. *Vet Dermatol* 12:303–13

Norris RA, Moreno-Rodriguez R, Hoffman S *et al.* (2009) The many facets of the matricelluar protein periostin during cardiac development, remodeling, and pathophysiology. *J Cell Commun Signal* 3:275–86

Numata Y, Terui T, Okuyama R *et al.* (2006) The accelerating effect of histamine on the cutaneous wound-healing process through the action of basic fibroblast growth factor. *J Invest Dermatol* 126:1403–9

Oka T, Xu J, Kaiser RA *et al.* (2007) Genetic manipulation of periostin expression reveals a role in cardiac hypertrophy and ventricular remodeling. *Circ Res* 101:313–21

Okamoto M, Hoshino T, Kitasato Y *et al.* (2011) Periostin, a matrix protein, is a novel biomarker for idiopathic interstitial pneumonias. *Eur Respir J* 37:1119–27

Oku E, Kanaji T, Takata Y *et al.* (2008) Periostin and bone marrow fibrosis. *Int J Hematol* 88:57–63

Ontsuka K, Kotobuki Y, Shiraishi H *et al.* (2012) Periostin, a matricellular protein, accelerates cutaneous wound repair by activating dermal fibroblasts. *Exp Dermatol* 21:331–6

Russel JD, Russell SB, Trupin KM (1977) The effect of histamine on the growth of cultured fibroblasts isolated from normal and keloid tissue. *J Cell Physiol* 93:389–93

Sandberg N (1962) Accelerated collagen formation and histamine. *Nature* 194:183

Sandberg N (1964) Enhanced rate of healing in rats with an increased rate of histamine formation. *Acta Chir Scand* 127:9–21

Shimazaki M, Kudo A (2008) Impaired capsule formation of tumors in periostin-null mice. *Biochem Biophys Res Commun* 367:736–42

Shimazaki M, Nakamura K, Kii I *et al.* (2008) Periostin is essential for cardiac healing after acute myocardial infarction. *J Exp Med* 205:295–303

Siriwardena BS, Kudo Y, Ogawa I *et al.* (2006) Periostin is frequently overexpressed and enhances invasion and angiogenesis in oral cancer. *Br J Cancer* 95:1396–403

Spector SL, Shikiar R, Harding G *et al.* (2007) The effect of fexofenadine hydrochloride on productivity and quality of life in patients with chronic idiopathic urticaria. *Cutis* 79:157–62

Takayama G, Arima K, Kanaji T *et al.* (2006) Periostin: a novel component of subepithelial fibrosis of bronchial asthma downstream of IL-4 and IL-13 signals. *J Allergy Clin Immunol* 118:98–104

Terao M, Murota H, Kitaba S *et al.* (2010) Tumor necrosis factor-alpha processing inhibitor-1 inhibits skin fibrosis in a bleomycin-induced murine model of scleroderma. *Exp Dermatol* 19:38–43

Thompson AK, Finn AF, Schoenwetter WF (2000) Effect of 60 mg twice-daily fexofenadine HCl on quality of life, work and classroom productivity, and regular activity in patients with chronic idiopathic urticaria. *J Am Acad Dermatol* 43:24–30

Topol BM, Lewis VL, Benveniste K (1981) The use of antihistamine to retard the growth of fibroblasts derived from human skin, scar, and keloid. *Plast Reconstr Surg* 68:227–32

Trautmann A, Toksoy A, Engelhardt E *et al.* (2000) Mast cell involvement in normal human skin wound healing: expression of monocyte chemoattractant protein-1 is correlated with recruitment of mast cells which synthesize interleukin-4 *in vivo*. *J Pathol* 190:100–6

Wahlgren CF (1999) Itch and atopic dermatitis: an overview. *J Dermatol* 26:770–9

Weller K, Foitzik K, Paus R *et al.* (2006) Mast cells are required for normal healing of skin wounds in mice. *FASEB J* 20:2366–8

Wood SH, Clements DN, Ollier WE *et al.* (2009a) Gene expression in canine atopic dermatitis and correlation with clinical severity scores. *J Dermatol Sci* 55:27–33

Wood SH, Ke X, Nuttall T *et al.* (2009b) Genome-wide association analysis of canine atopic dermatitis and identification of disease related SNPs. *Immunogenetics* 61:765–72

Yang L, Serada S, Fujimoto M *et al.* (2012) Periostin facilitates skin sclerosis via PI3K/Akt dependent mechanism in a mouse model of scleroderma. *PLoS One* 7:e41994

IJC
International Journal of Cancer

Annexin A4-conferred platinum resistance is mediated by the copper transporter ATP7A

Shinya Matsuzaki[1,2], Takayuki Enomoto[3], Satoshi Serada[2], Kiyoshi Yoshino[1], Shushi Nagamori[4], Akiko Morimoto[1], Takuhei Yokoyama[1,2], Ayako Kim[2], Toshihiro Kimura[1], Yutaka Ueda[1], Masami Fujita[1], Minoru Fujimoto[2], Yoshikatsu Kanai[4], Tadashi Kimura[1] and Tetsuji Naka[2]

[1] Department of Obstetrics and Gynecology, Osaka University Graduate School of Medicine, Osaka, Japan
[2] Laboratory for Immune Signal, National Institute of Biomedical Innovation, Osaka, Japan
[3] Department of Obstetrics and Gynecology, Niigata University Graduate School of Medicine, Niigata, Japan
[4] Department of Pharmacology, Osaka University Graduate School of Medicine, Osaka, Japan

Although platinum drugs are often used for the chemotherapy of human cancers, platinum resistance is a major issue and may preclude their use in some cases. We recently reported that enhanced expression of Annexin A4 (Anx A4) increases chemoresistance to carboplatin through increased extracellular efflux of the drug. However, the precise mechanisms underlying that chemoresistance and the relationship of Anx A4 to platinum resistance *in vivo* remain unclear. In this report, the *in vitro* mechanism of platinum resistance induced by Anx A4 was investigated in endometrial carcinoma cells (HEC1 cells) with low expression of Anx A4. Forced expression of Anx A4 in HEC1 cells resulted in chemoresistance to platinum drugs. In addition, HEC1 control cells were compared with Anx A4-overexpressing HEC1 cells in xenografted mice. Significantly greater chemoresistance to cisplatin was observed *in vivo* in Anx A4-overexpressing xenografted mice. Immunofluorescence analysis revealed that exposure to platinum drugs induced relocation of Anx A4 from the cytoplasm to the cellular membrane, where it became colocalized with ATP7A, a copper transporter also well known as a mechanism of platinum efflux. ATP7A expression suppressed by small interfering RNA had no effect on HEC1 control cells in terms of chemosensitivity to platinum drugs. However, suppression of ATP7A in Anx A4-overexpressing platinum-resistant cells improved chemosensitivity to platinum drugs (but not to 5-fluorouracil) to a level comparable to that of control cells. These results indicate that enhanced expression of Anx A4 confers platinum resistance by promoting efflux of platinum drugs *via* ATP7A.

Platinum drugs, widely used for treating gynecological cancers, can improve survival rates dramatically, particularly in patients with ovarian and endometrial carcinomas.[1–6] Compared with platinum-sensitive tumors, prognosis is poorer for tumors that are (or become) platinum-resistant; for these tumors, other chemotherapeutic drugs also tend to be less effective. For example, an efficacy of 81% has been demonstrated for chemotherapy regimens that include platinum drugs for treatment of ovarian serous adenocarcinoma (SAC), the most common subtype of ovarian carcinoma; however, the efficacy of these regimens is only 18% for ovarian clear cell carcinomas (CCC), which are frequently resistant to multiple drugs.[7] Compared with advanced SAC, the clinical prognosis of patients with similarly advanced CCC is markedly worse largely because of the considerably higher rate of recurrence after CCC treatment.[7–11] Therefore, determining the mechanism underlying platinum resistance may aid in identification of therapeutic targets for platinum-resistant tumors such as CCC. Studies using proteomic screening approaches have previously demonstrated overexpression of Annexin A4 (Anx A4) protein in ovarian CCC, which is frequently a highly platinum-resistant tumor compared with SAC.[12] Similar findings have been reported in a study comparing SAC and CCC using a genomic screening approach.[13] Anx A4, a previously understudied member of the Annexin protein family, binds to phospholipids in a Ca^{2+}-dependent manner, self-associates on phospholipid

Key words: Annexin A4, ATP7A, platinum resistance, platinum transporter, copper transporter
Abbreviations: 5-FU: 5-fluorouracil; Anx A4: Annexin A4; CCC: clear cell carcinoma; D-MEM: Dulbecco's modified Eagle's medium; FBS: fetal bovine serum; PBS: phosphate-buffered saline; SAC: serous adenocarcinoma; siRNA: small interfering RNA
Additional Supporting Information may be found in the online version of this article.
Grant sponsor: Japanese Ministry of Education, Science, Culture and Sports; **Grant number:** 22791560; **Grant sponsors:** Program for Promotion of Fundamental Studies in Health Sciences of the National Institute of Biomedical Innovation, Ministry of Health, Labour and Welfare of Japan
DOI: 10.1002/ijc.28526
History: Received 4 Dec 2012; Accepted 26 Sep 2013; Online 8 Oct 2013
Correspondence to: Dr. Tetsuji Naka, Laboratory for Immune Signal, National Institute of Biomedical Innovation, 7-6-8 Saito-asagi, Ibaraki, Osaka 567-0085, Japan, Tel.: +81-72-641-9843, Fax: +81-72-641–9837, E-mail: tnaka@nibio.go.jp

What's new?

Although platinum-based drugs are often used in chemotherapy, resistance to these drugs is frequently a problem. The protein Annexin A4 (Anx A4) is known to be involved in platinum efflux in ovarian tumours; however, its precise mechanism of action has been unclear. In this study, the authors demonstrated that the strong platinum-resistance in Anx A4-overexpressing cells involves the transporter protein ATP7A, both in vitro and in vivo. This suggests that Anx A4 may be a highly useful therapeutic target in Anx A4-expressing carcinomas.

membrane surfaces and causes membrane aggregation.[12,14–17] Enhanced expression of Anx A4 has recently shown to increase tumor chemoresistance to carboplatin (a key drug for treating gynecological cancers) *via* increased extracellular efflux of the drug.[12] Another study showed that Anx A4 suppresses NF-κB transcriptional activity, which is significantly upregulated early after etoposide treatment. Anx A4 translocates to the nucleus together with p50 and imparts greater resistance to apoptotic stimulation by etoposide treatment.[18] Anx A4 may also be associated with drug resistance in other types of tumors; enhanced expression of Anx A4 has been reported in colon, renal, lung and pancreatic cancers.[19–23] However, the details of Anx A4-mediated extracellular efflux of platinum drugs remain unclear.

HEC1 is an endometrial carcinoma cell line with low Anx A4 expression levels. In our study, Anx A4-overexpressing derivative HEC1 cell lines were established and their chemosensitivity toward platinum drugs was analyzed both *in vitro* and *in vivo*. Anx A4-conferred platinum chemoresistance was shown to be mediated by the copper transporter ATP7A.[24–28]

Material and Methods

Cell lines

The human endometrial carcinoma cell lines HEC1, HEC1A, HEC6, HEC88nu, HEC108, HEC116 and HEC251; SNGII and SNGM cells, the human ovarian SAC cell line OVSAHO and the ovarian CCC cell lines OVISE and OVTOKO were obtained from the Japanese Collection of Research Bioresources (Osaka, Japan); A2780 cells from the human ovarian SAC cell line were obtained from the European Collection of Animal Cell Culture (Salisbury, Scotland). The identity of each cell line was confirmed by DNA fingerprinting *via* short tandem repeat profiling, as described previously.[29] HEC1, HEC1A, HEC6, HEC88nu, HEC108, HEC116 and HEC251 cells were maintained in Dulbecco's modified Eagle's medium (D-MEM) (Wako Pure Chemical Industries, Osaka, Japan) supplemented with 10% fetal bovine serum (FBS) (HyClone Laboratories, Logan, UT) and 1% penicillin–streptomycin (Nacalai Tesque, Kyoto, Japan) at 37°C under a humidified atmosphere of 5% CO_2. SNGII and SNGM cells were maintained in Ham's F12 medium (Invitrogen, Carlsbad, CA) supplemented with 10% FBS and 1% penicillin–streptomycin. OVSAHO, A2780, OVISE and OVTOKO cells were maintained in Roswell Park Memorial Institute 1640 medium (Wako Pure Chemical Industries) supplemented with 10% FBS and 1% penicillin–streptomycin.

Generation of Anx A4 stably transfected cell lines

To generate cell lines that stably expressed Anx A4, HEC1 cells were transfected with the pcDNA3.1–Anx A4 expression plasmid, as described previously.[12] Transfected cells were selected with 600 μg/ml of Geneticin (Invitrogen). Clones were maintained in 250 μg/ml of Geneticin for stability of expression. Four stable Anx A4-expressing cell lines were established and designated HEC1-A25, HEC1-A43, HEC1-A63 and HEC1-A77. A control cell line of HEC1 was also established and stably transfected with an empty vector. This cell line was designated as HEC1-CV.

Western blotting

Cells were lysed in radioimmunoprecipitation assay buffer [10 mM Tris-HCl, pH 7.5, 150 mM NaCl, 1% Nonidet P-40, 0.5% sodium deoxycholate, 0.1% sodium dodecyl sulfate, 1% protease-inhibitor cocktail (Nacalai Tesque) and 1% phosphatase-inhibitor cocktail (Nacalai Tesque)]. After centrifugation (13,200 rpm, 4°C, 15 min), soluble proteins in the supernatant were separated using sodium dodecyl sulfate-polyacrylamide gel electrophoresis, as described previously.[12] Additional information can be found in Supporting Information Material and Methods.

Measurement of IC_{50} values after treatment with cisplatin or carboplatin

Cells were suspended in D-MEM medium supplemented with 10% FBS and were seeded in 96-well plates (2,000 cells per well) (Costar; Corning, Corning, NY) for 24 hr. They were then exposed to various concentrations of carboplatin (0–500 μM), cisplatin (0–100 μM) or 5-fluorouracil (5-FU) (0–50 μM) for 72 hr. Cell proliferation was evaluated using the WST-8 assay (Cell Counting Kit-SF; Nacalai Tesque) after treatment at the time points indicated by the manufacturer. The absorption of WST-8 was measured at a wavelength of 450 nm (reference wavelength: 630 nm) using a Model 680 microplate reader (Bio-Rad Laboratories, Hercules, CA). Absorbance values for treated cells indicative of proliferation rates were expressed as percentages relative to results for untreated controls, and the drug concentrations resulting in a 50% inhibition of cell growth (IC_{50} values) were calculated.

Small interfering RNA transfection

Two commercial small interfering RNAs (siRNAs) against ATP7A and a nonspecific control siRNA were obtained from

Qiagen (Venlo, The Netherlands) and designated ATP7A siRNA4 and ATP7A siRNA6, respectively. For gene silencing, a specific sense strand 5′-GCAGCUUGUAGUAUUGAA ATT-3′ was used for ATP7A siRNA4, and an antisense strand 5′-UUUCAAUACUACAAGCUGCTA-3′ was also used. For ATP7A siRNA6, a specific sense strand 5′-GCGUA GCUCCAGAGGUUUATT-3′ was used, and an antisense strand 5′-UAAACCUCUGGAGCUACGCAG-3′ was also used. Cells were transfected with siRNA using Lipofectamine 2000 reagent (Invitrogen) according to the manufacturer's instructions. Selective silencing of ATP7A was confirmed by Western blot analysis.

In vivo model of cisplatin resistance

All animal experiments were conducted in accordance with the Institutional Ethical Guidelines for Animal Experimentation of our National Institute of Biomedical Innovation (Osaka, Japan). Four-week-old, female Institute of Cancer Research (ICR) nu/nu mice were obtained from Charles River Japan (Yokohama, Japan). For subcutaneous xenograft experiments, 2.5×10^6 HEC1, HEC1-CV, HEC1-A63 and HEC1-A77 cells were suspended in 100 μl of 1/1 (v/v) phosphate-buffered saline (PBS)/Matrigel (Becton Dickinson, Bedford, MA) and injected subcutaneously into the flanks of the ICR nu/nu mice ($n = 5$ per group). One week after xenograft establishment, tumors measured ~100 mm^3. Mice were then randomly divided into two groups and administered cisplatin (3 mg/kg) or PBS i.p. twice weekly for 4 weeks. Tumor volumes were determined twice weekly by measuring length (L), width (W) and depth (D). Tumor volume was calculated using the formula: tumor volume (mm^3) = $W \times L \times D$. At 56 days after tumor implantation, tumors were removed and weighed.

Quantification of intracellular platinum accumulation

Cisplatin accumulation in cells was analyzed according to a previously established method, with certain minor modifications. In brief, 6×10^6 cells (HEC1, HEC1-CV, HEC1-A25, HEC1-A43, HEC1-A63 and HEC1-A77 cells) were seeded into two 150-mm tissue culture dishes and incubated for 24 hr. The cells were then exposed to 1 mM cisplatin for 60 min at 37°C and then washed twice with PBS. After 3 hr of incubation in cisplatin-free D-MEM medium (supplemented with 10% FBS), whole extracts were prepared and the concentration of intracellular platinum was determined using an Agilent 7500ce inductively coupled plasma mass spectrometer (ICP-MS; Agilent, Santa Clara, CA). The absolute concentration of platinum in each sample was determined from a calibration curve prepared with a platinum standard solution.

Preparation of crude membrane fractions

To investigate the localization of Anx A4, crude membrane fractions (CMFs) of cells treated in various ways were prepared. Cells were divided into three groups: those that received no treatment, those pretreated with 10 μM cisplatin for 4 hr and those pretreated with 50 μM carboplatin for 4 hr. CMF were prepared as described elsewhere,[30] with modifications. Prepared proteins were investigated using Western blot analysis. Additional information can be found in Supporting Information Material and Methods.

Biotinylation of HEC1 cell membrane surface proteins after cisplatin or carboplatin exposure

To investigate the localization of ATP7A after exposure to platinum drugs, treated or mock-treated HEC1 cells were surface-biotinylated and the presence of ATP7A was investigated by Western blot analysis. Additional information can be found in Supporting Information Material and Methods.

Immunofluorescence for ATP7A and Anx A4

Immunofluorescence staining was performed 2 days after cells had been seeded on cover slips. Before staining, cells in the treatment groups were pretreated with 10 μM cisplatin or 50 μM carboplatin for 4 hr. Cells were then analyzed for localization of Anx A4 and ATP7A. Additional information can be found in Supporting Information Material and Methods.

Statistical analysis

Statistical analyses were performed using one-way analysis of variance (ANOVA) followed by Dunnett's analysis to evaluate the significance of differences. In all analyses, $p < 0.05$ was considered to be statistically significant.

Results

Expression of Anx A4 in endometrial carcinoma cell lines

To investigate Anx A4 expression in nine common endometrial carcinoma cell lines, Western blot analyses were performed. Expression of Anx A4 was strongest in SNGM cells compared with the other eight cell lines (Fig. 1*a*). Thus, enhanced expression of Anx A4 was confirmed in this endometrial carcinoma cell line.

Anx A4 and platinum resistance in HEC1 cell lines

From control HEC1 cells (low Anx A4 expression levels), four stable lines of Anx A4-overexpressing cells (HEC1-A25, HEC1-A43, HEC1-A63 and HEC1-A77 cells) and one line of empty vector transfected cells (HEC1-CV cells) were established. Overexpression of Anx A4 was confirmed using Western blot analysis and was compared with CCC cell lines (OVTOKO and OVISE) used as positive controls (Fig. 1*b*). Significantly higher IC_{50} values for cisplatin were observed in HEC1-A25 (32.1 μM, $p < 0.01$), HEC1-A43 (23.8 μM, $p < 0.01$), HEC1-A63 (34.9 μM, $p < 0.01$) and HEC1-A77 cells (17.3 μM, $p < 0.01$) compared with HEC1 (9.8 μM) and HEC1-CV cells (8.4 μM) (Fig. 1*c*). Similarly, IC_{50} values for carboplatin were significantly increased in HEC1-A25 (194.6 μM, $p < 0.01$), HEC1-A43 (153.3 μM, $p < 0.01$), HEC1-A63 (371.5 μM, $p < 0.01$) and HEC1-A77 cells (158.1 μM, $p < 0.01$) compared with HEC1 (59.1 μM) and HEC1-CV cells (60.9 μM) (Fig. 1*c*). Thus, Anx A4 overexpression conferred platinum resistance in HEC1 cell lines.